


# TRPV1 gain-of-function mutation impairs pain and itch sensations in mice

Lina Duo<sup>1,2,3</sup> , Linghan Hu<sup>1,2,3</sup>, Naxi Tian<sup>4</sup>, Gen Cheng<sup>4</sup>,  
Huijun Wang<sup>1,2,3</sup>, Zhimiao Lin<sup>1</sup>, Yun Wang<sup>4</sup> and Yong Yang<sup>1,2,3</sup>

Molecular Pain  
Volume 14: 1–13  
© The Author(s) 2018  
Reprints and permissions:  
sagepub.com/journalsPermissions.nav  
DOI: 10.1177/1744806918762031  
journals.sagepub.com/home/mpx



## Abstract

Transient receptor potential vanilloid 1 (TRPV1) is a non-selective cation channel, which can detect various noxious stimuli that cause pain, inflammation, hyperalgesia, and itch. *TRPV1* knock-out mice show deficiency in nociception, but the in vivo effects of persistent activation of TRPV1 are not completely understood. Here, we generated *TRPV1* knock-in mice with a G564S mutation. In the heterologous expression system, an electrophysiological study showed that the G564S mutation in mouse TRPV1 caused increased basal current and a leftward shift of voltage dependence. Intriguingly, using behavioral analysis, we found that knock-in mice showed a thermosensory defect, impaired inflammatory thermal pain, and capsaicin sensitivity. We also demonstrated an attenuated behavioral response to the pruritic agent histamine in the knock-in mice. Indeed, calcium imaging together with electrophysiology showed that the overactive mutant had decreased capsaicin sensitivity. Western blot analysis revealed that the G564S mutant reduced TRPV1 phosphorylation and cell membrane trafficking. Together, we have generated a mouse model with a gain-of-function mutation in *Trpv1* gene and demonstrated that the pain and histamine-dependent itch sensations in these mice are impaired due to a decreased phosphorylation level and reduced membrane localization of TRPV1.

## Keywords

Transient receptor potential vanilloid 1, gain of function, pain, itch, phosphorylation, trafficking

Date Received: 27 September 2017; revised 10 January 2018; accepted: 21 January 2018

## Introduction

Capsaicin, the pungent ingredient of chili peppers, elicits hot and painful sensations by stimulating the nociceptors in mammals.<sup>1</sup> Originally identified as the molecular target of capsaicin, transient receptor potential vanilloid 1 (TRPV1) is a non-selective cation channel that responds to multiple noxious stimuli.<sup>2</sup> Besides pungent vanilloids like capsaicin, TRPV1 is also activated by noxious heat (>43°C) and acidic pH (<6.8).<sup>2,3</sup> Furthermore, TRPV1 shows considerable voltage dependence and is even considered to be directly activated by membrane depolarization (>60 mV) in the absence of any agonist.<sup>4</sup> Extensive studies have indicated that different stimuli usually act synergistically, that is, capsaicin, heat, protons, and voltage can enhance the efficacy and/or potency of one another.<sup>3,4</sup> This polymodal gating of TRPV1 is regarded as the essential mechanism underlying the function of nociceptive neurons.

<sup>1</sup>Beijing Key Laboratory of Molecular Diagnosis on Dermatoses, Department of Dermatology, Peking University First Hospital, Beijing, China

<sup>2</sup>Peking-Tsinghua Center for Life Sciences, Beijing, China

<sup>3</sup>Academy for Advanced Interdisciplinary Studies, Peking University, Beijing, China

<sup>4</sup>The Key Laboratory for Neuroscience of the Ministry of Education and Health, Department of Neurobiology, School of Basic Medical Sciences, Neuroscience Research Institute, Peking University, Beijing, China

The first two authors contributed equally to this work.

## Corresponding Authors:

Yong Yang, Peking University First Hospital, No. 8, Xishiku Street, Beijing 100034, China.

Email: dryongyang@bjmu.edu.cn

Yun Wang, Department of Neurobiology, Neuroscience Research Institute, Peking University, No. 38, Xueyuan Road, Beijing 100191, China.

Email: wangy66@bjmu.edu.cn



With a molecular structure analogous to that of voltage-gated Kv potassium channels, TRPV1, together with other members of the TRP subfamily, comprises four identical subunits, each of which includes six transmembrane (TM) domains (TM1–6): TM5–6 and the loop region between them form a cation-permeable pore, and TM1–4 are considered to harbor the voltage sensor and the binding sites of agonists like capsaicin.<sup>5</sup> Similar to Kv channels, the linker region of TM4–5 plays a critical role in the allosteric coupling between channel domains and converts the conformational changes of TM1–4 into gating of the pore (Figure 1(a)).<sup>6</sup> Indeed, our previous study showed that the point mutations at G573 within the TM4–5 linker of another TRPV member—TRPV3—render the channel spontaneously active, thus causing the autosomal dominant disorder Olmsted syndrome in humans.<sup>7</sup> Moreover, several recent studies have indicated that when G563 of rat TRPV1, corresponding to G573 of TRPV3 (Figure 1(a)), is substituted by serine (G563S), the mutated TRPV1 channel displays a shift of voltage-dependent activation to less depolarizing potentials, an increased basal current, and a stabilized open conformation.<sup>8</sup> All these phenotypes of the rat TRPV1 G563S mutant resemble the gain-of-function mutations of TRPV3.

Although previous functional studies of TRPV1-null mice have revealed significantly impaired nociceptive transduction and pain sensation, the deficiency appears to be limited to the sensory system.<sup>9,10</sup> Much the same as the knock-out of TRPV1, the knock-out of TRPV3 also causes minor defects in thermosensation.<sup>11</sup> However, gain-of-function mutations of TRPV3 lead to severe phenotypes, so it would be intriguing to ask whether similar substitutions of the corresponding TRPV1 amino-acid residue result in severe diseases, thereby revealing more aspects of TRPV1 function and possibly establishing its association with certain human diseases. Therefore, in this study, we explored the possible physiological abnormalities caused by a gain-of-function mutation of TRPV1 using a genetic strategy to generate the TRPV1 G564S knock-in mice (TRPV3 G573 corresponds to mouse TRPV1 G564, see Figure 1(a)).

## Materials and methods

### Animals

TRPV1 G564S knock-in mice in the C57BL/6N background were generated by the Cyagen Company (Guangzhou, China). In brief, construction of the

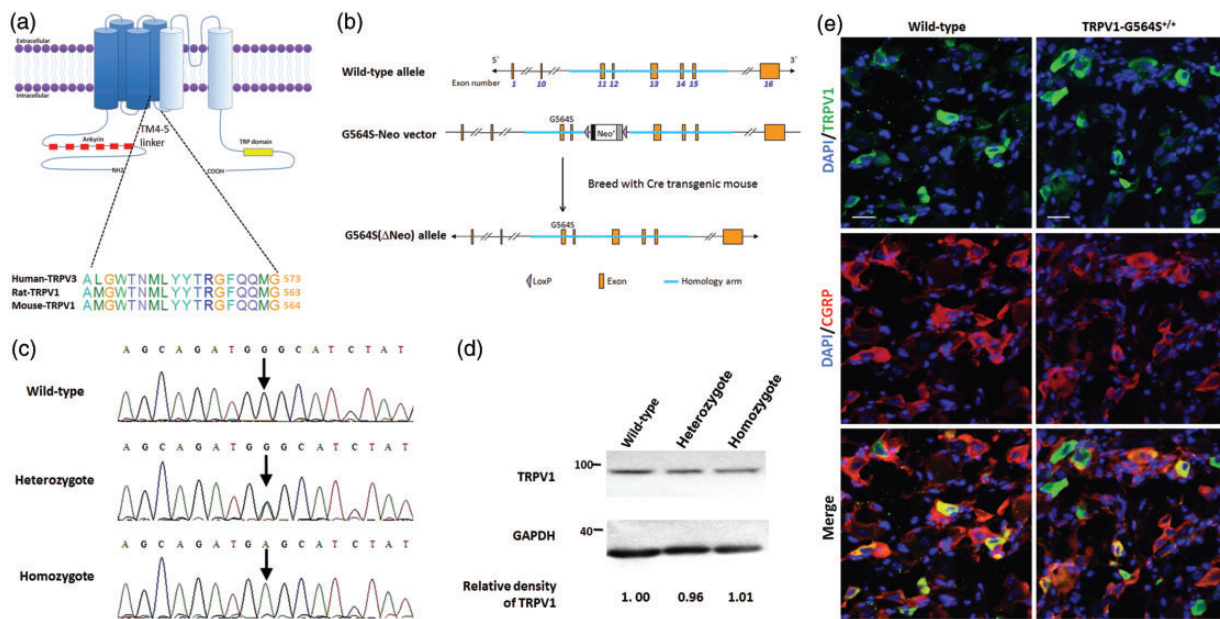


**Figure 1.** Generation and characterization of TRPV1 G564S knock-in mice. (a) Topology of the TRPV1 channel subunit and homology between TRPV3 and TRPV1; (b) schematic of the domain structure of (upper) mouse *Trpv1* genomic loci, (middle) the construct showing fusion of the homologous arm containing G564S in exon 11 followed by the neo selection marker flanked by loxP sites, and (lower) a map of the G564S ( $\Delta$ Neo) allele; (c) gene sequence analysis identifying the genotype of a wild-type animal (upper), heterozygote (middle), and homozygote (lower); (d) representative Western blots of DRG tissue showing the comparative expression levels of TRPV1 in wild-type, heterozygotic, and homozygotic mice after normalizing to  $\beta$ -actin. Note the comparable relative densities of TRPV1 blots scaled to the wild type; (e) representative immunofluorescence staining of DRG sections revealing the comparable distribution of TRPV1 and colocalization with CGRP in TRPV1 G564S<sup>+/+</sup> mice (right) and wild-type controls (left). Scale bars, 20  $\mu$ m. TRPV: transient receptor potential vanilloid; GAPDH: glyceraldehyde-3-phosphate dehydrogenase; DAPI: 4', 6-diamidino-2-phenylindole; CGRP: calcitonin gene-related peptide.

TRPV1 G564S allele was based on gene targeting. A cDNA containing a specific mutation site with a loxP-flanked *neo* cassette was targeted to the locus encoding TRPV1 using homologous recombination (Figure 1(b)). The polymerase chain reaction (PCR) and a standard southern blot approach were used to verify the targeting to the TRPV1 locus. Targeted embryonic stem cell clones were used to produce chimeric animals using eight-cell-stage injection. The chimeric male mice with a neomycin selection cassette were mated with Cre females to obtain offspring and then inbred to develop the *Trpv1*<sup>G564S</sup>/N homozygous mice and their wild-type littermates. The *Trpv1*<sup>G564S</sup>/N homozygous mice without the *neo* cassette, referred to as TRPV1 G564S<sup>+/+</sup> mice, were used for all the experiments in this study. The wild-type littermate mice were used as controls. Animals were genotyped using primers as follows (5'-3'): forward, AATCGGTCTCTTTGCCTCTC; reverse, GACTAAAGCTGCGAGGATGGTGG. All animals were kept under a 12:12-h light/dark cycle at a room temperature of 23 ± 3°C and had free access to food and water. All animal procedures were approved by the Animal Care and Use Committee of Peking University First Hospital.

### Immunofluorescence

Adult male TRPV1 G564S<sup>+/+</sup> mice and their wild-type littermates were euthanized with CO<sub>2</sub>. Dorsal root ganglions (DRGs) (L4 to L5) were immediately removed, post-fixed in 4% paraformaldehyde at 4°C for 3 h, and then treated with 30% sucrose in phosphate-buffered saline (PBS) at 4°C for 24 h. The biopsies were then washed, embedded in Tissue-Tek OCT (Sakura Finetek, Tokyo, Japan), and cut on a freezing microtome. Mounted DRG sections (5 μm) were allowed to thaw to room temperature, treated with PBS containing 0.3% Triton X-100 for 15 min, and then blocked with 5% donkey serum for 1 h at 37°C. They were incubated with antibody to TRPV1 (goat, 1:50; Santa Cruz Biotechnology, Philadelphia, PA) and calcitonin gene-related peptide (CGRP; mouse, 1:200; Abcam, Cambridge, England) for 24 h followed by appropriate secondary antibodies that were labeled with either Alexa Fluor 488 (1:400; Jackson ImmunoResearch Laboratories, West Grove, PA) or Alexa Fluor 555 (1:500; Invitrogen, Carlsbad, CA) for 1 h. The stained sections were examined under an FV1000 laser scanning confocal microscope (OLYMPUS, Tokyo, Japan), and images were captured with a CCD spot camera.

### Western blot

Adult male TRPV1 G564S<sup>+/+</sup> mice and their wild-type littermates were euthanized with CO<sub>2</sub> and DRGs were

immediately removed and homogenized in RIPA lysis buffer containing protease and phosphatase inhibitors (Roche, Basel, Switzerland). The homogenate was rotated at 4°C for 20 min, centrifuged at 12,000 × g at 4°C for 15 min, and the supernatant was collected. The concentration of proteins was measured by the bicinchoninic acid method. Proteins from HEK293a cells were prepared as above. Crude protein extracts (40 μg) were denatured and separated on a Novex NuPAGE SDS-PAGE gel system (Invitrogen, Carlsbad, CA) as recommended by the manufacturer. After separation, protein was transferred onto polyvinylidene fluoride membranes (Merck Millipore, Boston, MA). The blots were blocked in 5% non-fat milk or 5% bovine serum albumin in Tris-buffered saline with Tween for 1 h at room temperature and incubated overnight at 4°C using antibody against TRPV1 (goat, 1:500; Santa Cruz Biotechnology, Philadelphia, PA), human influenza hemagglutinin (HA; mouse, 1:1000; Sigma-Aldrich, St. Louis, CA), anti-phosphoserine/threonine/tyrosine (mouse, 1:1000; Abcam, Cambridge, England), and β-actin (mouse, 1:2000; ZSGB-BIO, Beijing, China). These blots were further incubated with appropriate horseradish peroxidase-conjugated secondary antibodies and detected by an enhanced chemiluminescence kit (Merck Millipore). The density of the selected bands was quantified using ImageJ software (National Institutes of Health, Bethesda, MD).

### Behavioral analysis

All behavioral experiments were conducted on homozygous and littermate wild-type males aged 8–10 weeks. Animals were acclimated to the testing environment daily for three days before the experiment. Experimenters were blinded to the treatment or genotype of the mice during testing.

**Rotarod test.** To assess coordination and balance, mice were individually placed on the rotating Rotarod (LE8205; Panlab, Barcelona, Spain) for 60 s at 4 r/min, and subsequently, the speed was accelerated to 40 r/min in 10 min. The time to fall after the beginning of the acceleration was recorded. Each mouse received three test sessions with at least a 5-min interval between them, and the average time was calculated after discarding the lowest and highest.

**Capsaicin test.** The capsaicin test was performed as described previously.<sup>12</sup> After acclimatizing to the testing environment, the mouse was injected with 20 μl of capsaicin (1.6 μg/paw; Sigma-Aldrich) under the plantar surface of the left hindpaw. Each mouse was then put back in the observation cylinder and observed for 5 min. The sum of the time (s) spent in licking, biting, and shaking the injected paw was recorded as an indicator of the nociceptive response.



**Hot-plate test.** To assess heat sensitivity, mice were individually placed on a hot plate (YLS-6B; YiYan, Jinan, China) heated to 50°C, 52.5°C, 55°C, or 58°C and the latency (seconds) to the first sign of licking, shaking of hindpaws, or jumping was recorded. In order to avoid potential injury, mice were removed from the plate immediately after a nociceptive response or a cut-off time of 30 s. Each mouse was tested in five trials at least 5-min intervals. The mean time was calculated from the three values remaining after discarding the lowest and highest. Each day the mice were tested for one temperature in order to avoid habituation.

**Tail-flick test.** This test was performed at 26, 30, 34, or 38 W using a tail-flick unit (YLS-12A; YiYan). Mice were immobilized with a black cloth, and the tip of the tail (1/3 of the length) was laid on the infrared light bulb. The time (s) to withdrawal of the tail from the radiant heat source was measured. To prevent tissue damage, the cut-off time was kept at 16 s. Each mouse was tested in five trials at minimum intervals of 5 min. The mean time, excluding the highest and lowest values, was calculated. The mice were tested for one heat intensity per day in order to avoid habituation.

**Complete Freund's adjuvant test.** The basal heat sensitivity of animals was measured by a hot-plate test at 52.5°C before Complete Freund's adjuvant (CFA) administration. CFA (10  $\mu$ l, Sigma-Aldrich) was then injected into the left hindpaw. Heat hyperalgesia was assessed at 1, 2, 6, and 12 h and for one, three, and seven days after CFA injection.

**Acute scratching behavior.** Scratching behavior was assessed as previously described.<sup>13</sup> Briefly, one day after shaving the rostral back of the neck, mice were placed individually in plastic cages (19 cm  $\times$  29 cm  $\times$  15 cm) for at least 30 min to acclimate and intradermally injected in the rostral back of the neck with histamine (2.5  $\mu$ mol in 50  $\mu$ l of PBS; Sigma-Aldrich), chloroquine (200  $\mu$ g in 50  $\mu$ l of PBS; Sigma-Aldrich), endothelin 1 (ET-1; 25 ng in 50  $\mu$ l of PBS; Sigma-Aldrich),  $\alpha$ -methyl-5-hydroxytryptamine (5-HT; 30  $\mu$ g in 50  $\mu$ l of PBS; Sigma-Aldrich), peptide SLIGRL-NH<sub>2</sub> (SLIGRL; 100  $\mu$ g in 50  $\mu$ l of PBS; Sigma-Aldrich), or compound 48/80 (30  $\mu$ g in 50  $\mu$ l of PBS; Sigma-Aldrich). Hindlimb scratching toward the area around the drug injection was observed for 30 min at 5-min intervals. One bout of scratching was defined as one lifting of the hindlimb toward the injection site followed by putting the limb back on the floor or to the mouth, regardless of how many scratching strokes occurred between the two movements. In the control group, the mice were injected intradermally with 50- $\mu$ l PBS.

### *TRPV1-expressing vector production and site-directed mutagenesis*

Mouse *Trpv1* cDNA was incorporated into the pEGFP-N1 vector encoding a C-terminal enhanced green fluorescent protein (eGFP) tag through BglII and KpnI. To construct the TRPV1 expression vectors containing an HA tag, pEGFP-N1-TRPV1 plasmid was amplified with the primers (5'-3'): forward, TCCAGATTACGCTTAAAGCGGCCGCGACTCTA; reverse, ACATCGTATGGATATTTCTCCCCTGGGGCCAT. PCR products were then digested by DpnI (ThermoFisher, Waltham, MA) and ligated with T4 ligase (TransGen Biotech, Beijing, China), thereby substituting the eGFP tag sequence with the HA sequence.

### *Cell culture and transient transfection*

HEK293a cells were routinely cultured in Dulbecco's modified Eagle's medium (DMEM) containing 10% fetal bovine serum (FBS; Gibco, Darmstadt Germany) and 1% penicillin/streptomycin and transfected with TRPV1 wild type or G564S mutant plasmids using Lipofectamine 3000 (Invitrogen) as in the operation manual. Cells were used for experiments 16–48 h after transfection.

### *Electrophysiology*

In HEK293a cells transfected with pEGFP-N1-TRPV1 or pEGFP-N1-TRPV1-G564S plasmids, we made patch-clamp recordings using an EPC10 amplifier (HEKA, Lambrecht, Germany) driven by PatchMaster software (HEKA) as previously described.<sup>7</sup> Signals were filtered using a 2.9-kHz low-pass Bessel filter. Electrodes were fabricated from glass capillaries with a P-97 micropipette puller (Sutter Instruments, Novato, CA), and those with resistances of 2–5 M $\Omega$  were used for experiments. Cell membrane capacitance values were monitored and used to calculate current densities. To ensure that recordings were from cells previously unexposed to the agonist, transfected cells were placed on small coverslips, and only one recording was performed on each coverslip. For inside-out patch recordings, both bath and pipette solutions contained (in mM) 130 NaCl, 3 HEPES, and 0.3 EGTA, adjusted to pH 7.4 with NaOH. Whole-cell recordings were performed with an extracellular control solution containing (in mM) 140 NaCl, 4 KCl, 2 CaCl<sub>2</sub>, 1 MgCl<sub>2</sub>, and 10 HEPES, adjusted to pH 7.4 with NaOH. Pipettes were filled with an intracellular solution containing (in mM) 130 KCl, 8 NaCl, 2 EGTA, 1 MgCl<sub>2</sub>, 1 CaCl<sub>2</sub>, 4 MgATP, and 0.4 Na<sub>2</sub>GTP, adjusted to pH 7.4 with CsOH. For experiments in Ca<sup>2+</sup>-free conditions, Ca<sup>2+</sup> was replaced with 2 mM EGTA in the extracellular solution (ES). All chemicals were from

Sigma-Aldrich. To examine TRPV1 activation by depolarization, a  $-70$  mV initial holding potential was applied, followed by a voltage step protocol consisting of 100-ms steps to test potentials ranging from  $-120$  mV to  $+180$  mV in 20-mV increments. Steady state currents at the end of 100-ms voltage steps were used to estimate the voltage-dependent gating parameters by fitting the normalized channel conductance ( $G/G_{\max}$ )–voltage relationship to a Boltzmann equation as follows:  $G/G_{\max} = G_{\min}/G_{\max} + ((G_{\max} - G_{\min})/G_{\max}(1 + \exp[-(V - V_{1/2})/k]))$ , where  $V_{1/2}$  is the half-activation voltage,  $G_{\min}$  and  $G_{\max}$  are the minimum and maximum whole-cell conductance, and  $k$  is the slope factor. All recordings were made at room temperature ( $24^{\circ}\text{C}$ ).

### Dissociated DRG neurons and calcium imaging

Acutely dissociated DRG neurons and Fura-2 acetoxy-methyl (Fura-2 AM)-based  $\text{Ca}^{2+}$  imaging experiments were performed as described previously.<sup>14</sup> TRPV1 G564S<sup>+/+</sup> mice and their wild-type littermates were terminally anesthetized with 10% chloral hydrate (0.3 g/kg, i.p.), and then the DRGs were removed and digested with collagenase-type IA (1.5 mg/ml; Sigma-Aldrich) for 50 to 60 min and then with 0.25% trypsin (Invitrogen) for 8 to 10 min at  $37^{\circ}\text{C}$ . The enzymatic treatment was terminated by the addition of 10% FBS followed by gentle trituration of the ganglia with a flame-polished Pasteur pipette, and the cells were centrifuged at 1000 r/min for 3 min. The pellet was then resuspended in DMEM. The dissociated cells were plated on poly-D-lysine-coated (100 mg/ml; Sigma-Aldrich) glass coverslips in 35-mm culture dishes with a 10-mm bottom well and kept for 1.5 h at  $37^{\circ}\text{C}$  in an incubator with 5%  $\text{CO}_2$  and 95% air.

The DRG cells were washed twice with ES (7.605 g NaCl, 0.3725 g KCl, 0.272 g  $\text{KH}_2\text{PO}_4$ , 0.094 g  $\text{MgCl}_2$ , 0.2775 g  $\text{CaCl}_2$ , 1.8 g glucose, and 2.38 g HEPES, dissolved in 1000 ml of ddH<sub>2</sub>O, pH 7.4 to 7.6, 300 mOsm) and then incubated in Fura-2 AM (5 mM; Invitrogen) in ES at room temperature for 40 min. The cells were then washed with ES and left in ES at room temperature in the dark for 1 h recovery. For calcium imaging, an inverted fluorescence microscope equipped with 340- and 380-nm excitation filters (Olympus) and a computer with MetaFluor software (Visitron, Puchheim, Germany) were used. Fluorescent images and the F340/F380 ratio were acquired every 5 s. TRPV1 activation was evoked by the addition of 1- $\mu\text{M}$  or 5- $\mu\text{M}$  capsaicin.

### Immunoprecipitation

Extracts of HEK293a cells transfected with HA-TRPV1 or HA-TRPV1-G564S plasmids were used for

immunoprecipitation following the operation manual of the Crosslink Magnetic IP/Co-IP Kit (Pierce, Holmdel, NJ). Extracts containing 10 g of protein were incubated overnight at  $4^{\circ}\text{C}$  with 10  $\mu\text{g}$  of anti-HA antibody.

### Cell surface biotinylation assay

HEK293a cells transfected with HA-TRPV1 or HA-TRPV1-G564S plasmids were biotinylated. The surface protein was isolated using a cell surface protein isolation kit (Pierce) as in the operation manual. The levels of total TRPV1 and surface channel were analyzed by Western blot with an anti-HA antibody as described above.

### Statistical analysis

All data are expressed as mean  $\pm$  Standard Error of Mean (SEM) except for Figure 5(b) whose data are showed as mean only. Statistical analysis was performed with SPSS 19.0 software (IBM, Chicago, MI), and  $p < 0.05$  was considered statistically significant. Two-tailed unpaired  $t$  test was used for comparing two groups. Analyses of Fura-2 calcium imaging for dissociated DRG neurons and behavioral responses to heat and inflammatory pain were performed by two-way repeated-measures analysis of variance (ANOVA) followed by Bonferroni's post hoc tests.

## Results

### Generation of TRPV1 G564S knock-in mice

We used homologous recombination to generate mice with the specific site mutation c.G1690A in *Trpv1*; this mutation led to a glycine-to-serine substitution at amino-acid 564. The DNA sequencing results for wild-type, heterozygous, and homozygous mice are shown in Figure 1(c). TRPV1 G564S<sup>+/+</sup> mice were normal in general appearance, gross anatomy, body weight, locomotion, and overt behavior. To determine whether the G564S mutation affects the TRPV1 expression in DRG neurons, we performed Western blotting to examine the protein levels of TRPV1 and found no significant difference in the expression between TRPV1 G564S knock-in mice and their wild-type littermates (Figure 1(d)). Immunostaining revealed that TRPV1 was selectively expressed in small- and medium-diameter neurons within DRGs and was highly colocalized with CGRP, consistent with previous reports. Moreover, there was no difference in cellular localization of TRPV1 between the genotype groups (Figure 1(e)). These results indicate that the G564S mutation does not change the expression and distribution of TRPV1 in DRG neurons.

### G564S mutation results in gain-of-function TRPV1 channels

To determine whether the G564S mutation in mouse TRPV1 increases channel activity, we made inside-out patch recordings in HEK293a cells co-expressing eGFP and either the TRPV1 wild-type channel or the G564S mutant. Capsaicin (1  $\mu$ M) applied to wild-type TRPV1 evoked a rapid, robust inward current, which was then

completely blocked by 130 mM  $Ba^{2+}$  from the intracellular side and returned almost to the initial basal current level; conversely, in the TRPV1 G564S mutant, the blocked current level was remarkably higher than the basal current level, suggesting that the G564S mutation leads to partial opening of TRPV1 channel before capsaicin stimulation (Figure 2(a)). Quantitative analysis showed that compared with wild-type TRPV1, the G564S mutant dramatically increased the ratio of the

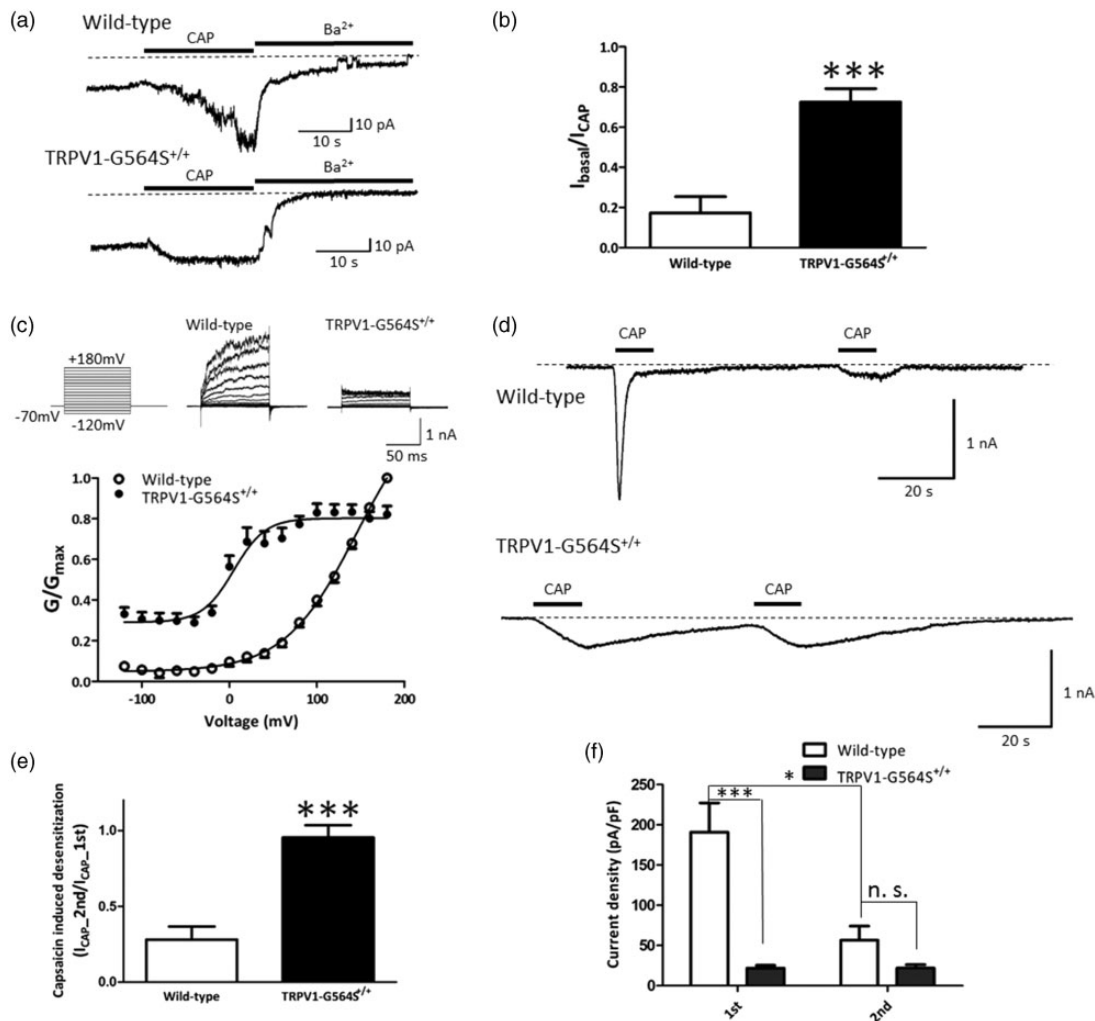


**Figure 2.** Electrophysiological recordings of wild-type TRPV1 and G564S mutant channels. (a) Representative currents from inside-out patches in HEK293a cells expressing wild-type TRPV1 (upper traces) and G564S mutant channels (lower traces) in response to stimulation by 1- $\mu$ M capsaicin (CAP) or inhibition by 130 mM  $Ba^{2+}$  to assess the level of leak currents at  $-70$  mV. Note that the G564S mutant channel showed little activation, then a dramatic block by  $Ba^{2+}$ . (b) Ratios of initial basal current amplitude to maximal current amplitude evoked by CAP in the TRPV1 wild-type and mutant channels ( $n = 7$ ,  $***p < 0.001$ , unpaired Student's  $t$  test). (c) Upper traces are representative whole-cell current traces in response to 100-ms voltage steps from  $-120$  mV to  $+180$  mV for wild-type TRPV1 and G564S mutant channels. Lower traces are normalized conductance-voltage relationships for wild-type TRPV1 and G564S mutants ( $n = 13-18$ ). Note the dramatic leftward shift of the G564S mutant channel. (d) Representative recordings of whole-cell current responses of HEK293a cells expressing wild-type TRPV1 (upper) or G564S mutant channels (lower) evoked by two consecutive applications of 1- $\mu$ M capsaicin at  $-70$  mV. The G564S mutant channels displayed no acute desensitization. (e) Current ratios of second to first CAP application for wild-type and mutant TRPV1 ( $n = 13-14$ ,  $***p < 0.001$ , unpaired Student's  $t$  test). (f) Inward current densities induced by first and second capsaicin application for wild-type and mutant TRPV1 ( $n = 13-14$ ,  $*p < 0.05$ ,  $***p < 0.001$ , unpaired Student's  $t$  test). TRPV: transient receptor potential vanilloid.

initial basal current to the maximal response induced by capsaicin (wild type,  $0.17 \pm 0.08$ ,  $n = 7$ ; G564S,  $0.73 \pm 0.07$ ,  $n = 7$ ;  $p < 0.001$ , unpaired  $t$  test; Figure 2(b)), suggesting that the G564S mutant acts in a gain-of-function manner.

We further characterized the G564S mutant using the whole-cell patch-clamp in HEK293a cells. Consistent with the findings for the rat TRPV1 G563S channel, the G564S mutation in mouse TRPV1 resulted in channels with a conductance-to-voltage relationship shifted toward less depolarizing potentials (Figure 2(c);  $V_{1/2}$  was  $145.5 \pm 9.2$  mV in the wild-type TRPV1 and  $5.0 \pm 4.9$  mV in the G564S mutant), indicating that the G564S mutant displays an elevated channel activity under physiological potentials.

Prolonged or repeated activation of TRPV1 results in desensitization, a state characterized by insensitivity of the receptor to subsequent stimuli. We repeated brief ( $\sim 10$  s long) applications of  $1\text{-}\mu\text{M}$  capsaicin at 1-min intervals in  $\text{Ca}^{2+}$ -containing (2 mM) bath solution and measured the current response. The wild-type TRPV1 showed strong tachyphylaxis, which occurred between the first and second applications of capsaicin, as described previously.<sup>15</sup> The mean current amplitude at the second capsaicin application was  $\sim 28\%$  that of the first application (Figure 2(d)). Unlike the TRPV1 wild-type channel, the TRPV1 G564S mutant displayed markedly slowed kinetics of the first capsaicin-induced response (Figure 2(d)), and the current amplitude at the second capsaicin application was comparable to that at the first application (wild-type,  $0.28 \pm 0.09$ ,  $n = 9$ ; G564S,  $0.95 \pm 0.08$ ,  $n = 13$ ;  $p < 0.001$ , unpaired  $t$  test; Figure 2(e)). These results imply the absence of desensitization in the TRPV1 G564S channel. Considering the dramatic difference in the mean current amplitude between groups at the first capsaicin application and the minor difference at the second capsaicin application

(Figure 2(f)), we speculate that the TRPV1 G564S channel may already be in a desensitized state due to channel hyperactivity.

We further validated the impact of the G564S mutation on channel activity *ex vivo*. Fura-2 AM  $\text{Ca}^{2+}$  imaging of acutely dissociated DRG neurons from TRPV1 G564S<sup>+/+</sup> mice and wild-type littermates showed that the G564S mutant increased the intracellular  $\text{Ca}^{2+}$  concentrations in the physiological state compared with wild-type TRPV1 (wild type,  $0.67 \pm 0.01$ ,  $n = 11$ ; G564S,  $0.88 \pm 0.05$ ,  $n = 9$ ;  $p < 0.001$ , unpaired  $t$  test; Figure 3(a)). Collectively, these *in vitro* and *ex vivo* studies demonstrate that the G564S mutation enhances TRPV1 activity and support the notion that we have generated a mouse model with gain-of-function TRPV1 channels.

### TRPV1 G564S mutation leads to reduced capsaicin response

Prior studies have shown that the TRPV1 agonist capsaicin induces nociceptive behavioral responses; therefore, we first evaluated the effects of the TRPV1 G564S mutation on behavioral measures of TRPV1 activity. We subcutaneously injected capsaicin into the plantar skin of the left hindpaw, and this stimulus led to robust licking and shaking responses toward the injected paw, whereas the time the animals spent licking and shaking the paw was markedly reduced in TRPV1 G564S<sup>+/+</sup> mice compared with wild-type controls (wild type,  $34.19 \pm 3.80$  s,  $n = 5$ ; TRPV1-G564S<sup>+/+</sup>,  $9.63 \pm 1.29$  s,  $n = 6$ ;  $p < 0.001$ , unpaired  $t$  test; Figure 4(a)), suggesting that the G564S mutation leads to reduced peripheral TRPV1 reactivity. To exclude the influence of motor defects on behavioral assessments, we also performed the rotarod test, which revealed a similar latency to fall in the wild-type and TRPV1 G564S<sup>+/+</sup> mice (wild

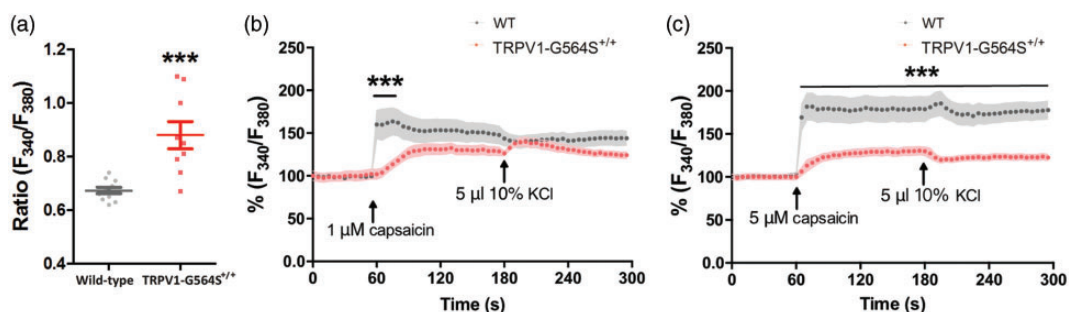


**Figure 3.** Attenuation of intracellular  $\text{Ca}^{2+}$  increase to capsaicin stimulation in neurons isolated from TRPV1 G564S<sup>+/+</sup> mice. (a) Basal intracellular  $\text{Ca}^{2+}$  concentrations (as F340/F380) in DRG neurons dissociated from TRPV1 G564S<sup>+/+</sup> mice and wild-type littermates ( $n = 9\text{--}11$  neurons, \*\*\* $p < 0.001$  compared with corresponding control group, unpaired Student's  $t$  test). (b, c) Intracellular  $\text{Ca}^{2+}$  responses to  $1\text{ }\mu\text{M}$  (b) or  $5\text{ }\mu\text{M}$  (c) capsaicin in DRG neurons dissociated from TRPV1 G564S<sup>+/+</sup> mice and wild-type littermates. Note the faster and more dramatic increase of  $\text{Ca}^{2+}$  signals in wild-type neurons. In (b) and (c), Fura-2 ratio was normalized to  $t_0$  in each group,  $n = 7\text{--}11$  neurons, \*\*\* $p < 0.001$  compared with corresponding control groups, two-way ANOVA, followed by Bonferroni post hoc tests. TRPV: transient receptor potential vanilloid; WT: wild type.



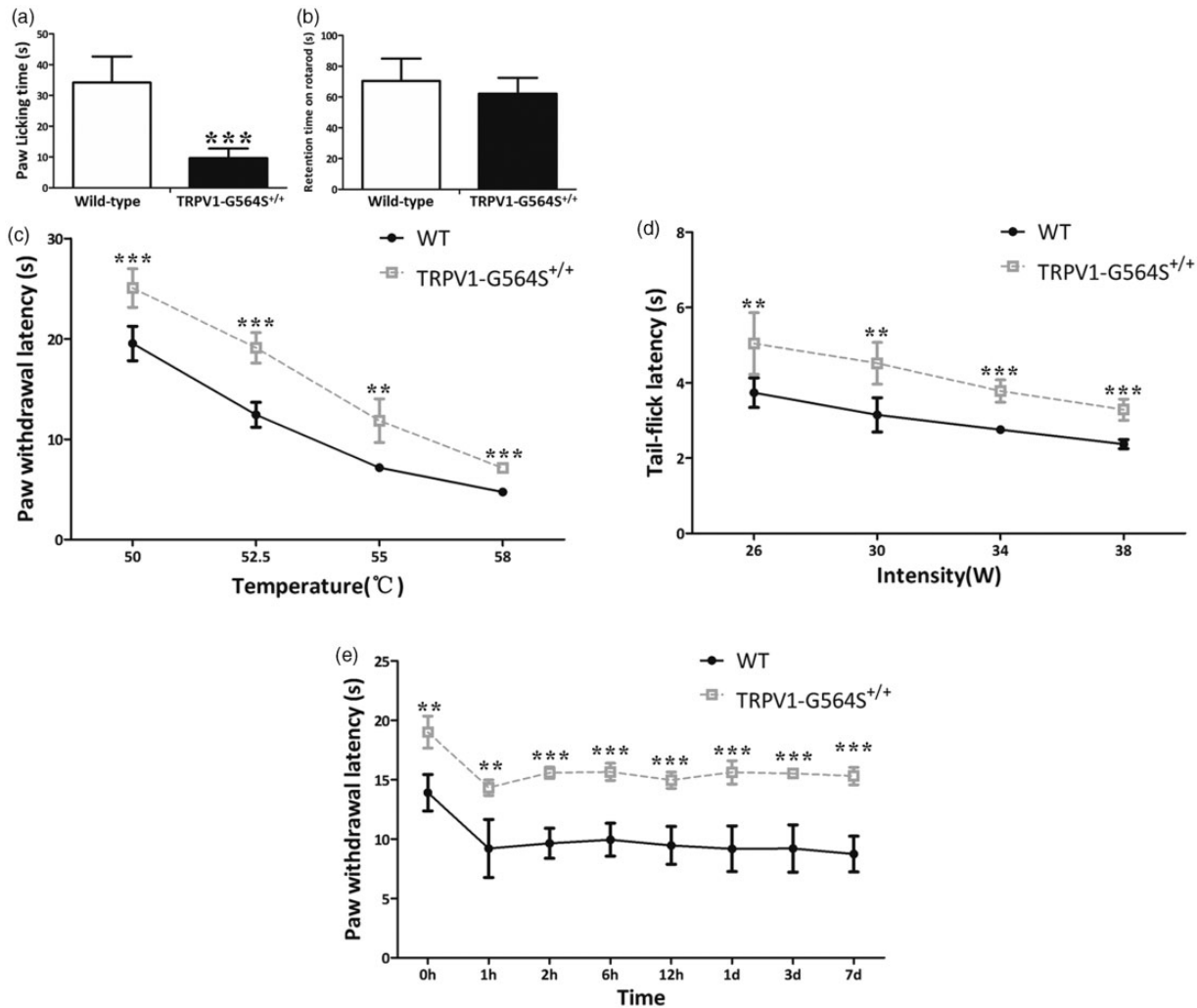


**Figure 4.** Impaired behavioral responses of TRPV1 G564S<sup>+/+</sup> mice to capsaicin, heat, and inflammatory pain. (a) Total duration of capsaicin-induced nociceptive responses during a 5-min period ( $n = 8-9$ ,  $***p < 0.001$ , unpaired Student's  $t$  test). (b) Latency to fall in the rotarod test was comparable between TRPV1 G564S<sup>+/+</sup> mice ( $n = 8$ ) and wild-type littermates ( $n = 6$ ). (c) Latency to paw withdrawal in the hot-plate test of TRPV1 G564S<sup>+/+</sup> mice ( $n = 8$ ) and wild-type littermates ( $n = 5$ ). Note the withdrawal latency of TRPV1 G564S<sup>+/+</sup> mice was always significantly higher than wild-type littermates. (d) Latency to tail withdrawal in the tail-flick test of TRPV1 G564S<sup>+/+</sup> mice ( $n = 8$ ) and wild-type littermates ( $n = 5$ ). Note the tail flick latency of TRPV1 G564S<sup>+/+</sup> mice was always significantly higher than wild-type littermates. (e) Change in paw withdrawal latency tested by the hot plate at 52.5°C after intraplantar injection of CFA ( $n = 5$ ). Note the paw withdrawal latency of TRPV1 G564S<sup>+/+</sup> mice was always significantly higher than wildtype littermates. In (c-e), Error bars, SEM;  $***p < 0.001$  compared with corresponding control groups, two-way ANOVA, followed by Bonferroni post hoc tests,  $**p < 0.01$ ,  $***p < 0.001$ . TRPV: transient receptor potential vanilloid; WT: wild type.

type,  $70.44 \pm 5.94$  s,  $n = 6$ ; TRPV1-G564S<sup>+/+</sup>,  $62.17 \pm 10.35$  s,  $n = 6$ ;  $p = 0.28$ , unpaired  $t$  test; Figure 4(b)), demonstrating that the G564S mutation in TRPV1 does not cause motor function defects.

To further investigate the potential mechanisms by which TRPV1 activity is suppressed, we acutely dissociated DRG neurons from TRPV1 G564S<sup>+/+</sup> mice and their wild-type littermates and subjected them to Fura-2 calcium imaging. Capsaicin (1  $\mu$ M or 5  $\mu$ M) significantly and rapidly evoked an increase in intracellular Ca<sup>2+</sup> concentration in neurons from wild-type controls, whereas neurons from TRPV1 G564S<sup>+/+</sup> mice showed

relatively weaker Ca<sup>2+</sup> increase (1- $\mu$ M capsaicin:  $p = 0.22$ , two-way ANOVA, post hoc,  $p < 0.001$ , Figure 3(b); 5- $\mu$ M capsaicin:  $p < 0.001$ , two-way ANOVA, post hoc,  $p < 0.001$ , Figure 3(c)). These results duplicated the difference revealed by whole-cell patch-clamp recording, wherein at the first capsaicin application, the mean current amplitude was significantly reduced in the G564S channel compared with wild-type TRPV1 channel (wild type,  $190.86 \pm 36.39$  pA/pF,  $n = 13$ ; G564S,  $22.73 \pm 3.72$  pA/pF,  $n = 14$ ;  $p < 0.001$ , unpaired  $t$  test; Figure 2(f)). In fact, the current amplitudes evoked by voltage steps were also smaller in the



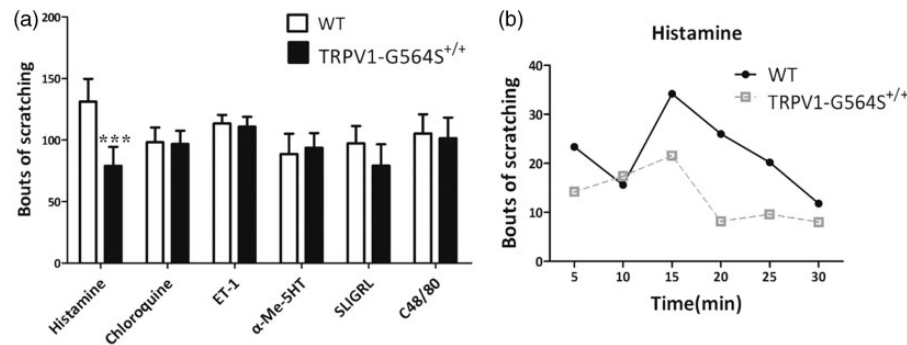


**Figure 5.** Impaired behavioral responses of TRPV1 G564S<sup>+/+</sup> mice to pruritic stimuli. (a) Bouts of scratching with hindlimbs during 30 min induced by intradermal pruritogen injection. Error bars, SEM; n = 5–8; \*\*\*P < 0.001, unpaired Student's *t* test. (b) Time course of histamine-induced scratching following intradermal injection of 2.5- $\mu$ mol histamine into TRPV1 G564S<sup>+/+</sup> mice and wild-type controls (n = 5). TRPV: transient receptor potential vanilloid; WT: wild type; ET-1: endothelin I; 5HT: 5-hydroxytryptamine; SLIGRL: peptide SLIGRL-NH<sub>2</sub>; C48/80: compound 48/80.

G564S channel than in wild-type TRPV1 channel (Figure 2(c)). These results show that the gain-of-function mutation in TRPV1 reduces the overall reactivity to capsaicin *ex vivo* and *in vitro*.

#### *TRPV1 G564S knock-in mice display a reduced sensitivity to acute thermal pain*

Knowing that TRPV1 is activated by pain-causing stimuli to induce nociception, we then characterized the phenotypic sensory properties of TRPV1 G564S<sup>+/+</sup> mice. TRPV1 is activated by noxious heat (>43°C) to evoke pain in humans or pain-related behaviors in animals. To assess the role of the TRPV1 G564S mutation in heat sensitivity, we investigated whether acute thermal pain is changed in the TRPV1 G564S<sup>+/+</sup> mice using the hot-plate and tail-flick tests. The hot-plate test revealed that the response latency at four different noxious temperatures was substantially prolonged in TRPV1 G564S<sup>+/+</sup> mice than in wild-type mice (Figure 4(c)). Consistently, TRPV1 G564S<sup>+/+</sup> mice exhibited prolonged tail-flick latencies at all tested intensities (Figure 4(d)). Together, these data reveal an intriguing phenotype in TRPV1 G564S<sup>+/+</sup> mice: a reduced acute thermal sensitivity.

#### *TRPV1 G564S knock-in mice show impaired thermal hyperalgesia during inflammation*

CFA induces rapid (one day) and persistent (>seven days) heat hyperalgesia. To determine the contribution of the TRPV1 G564S mutation to inflammatory pain, we injected CFA into the plantar surface of the left hindpaw of TRPV1 G564S<sup>+/+</sup> mice and their wild-type littermates to induce inflammation and evaluated the heat hyperalgesia from 1 to 12 h and over one to seven days after the injection of CFA using the hot-plate test. The basal heat sensitivity was tested before CFA

injection. CFA-induced inflammatory thermal hyperalgesia resulted in a significantly decreased paw-withdrawal latency in the wild-type mice in response to a 52.5°C heat stimulus, which persisted for seven days after CFA administration (Figure 4(e)). However, in the TRPV1 G564S<sup>+/+</sup> mice, inflammation-induced thermal hyperalgesia was relatively attenuated, as the withdrawal latency declined less from the basal heat-evoked latency at all time points tested after CFA administration. Together, these data suggest that the G564S mutation alleviates thermal hyperalgesia during inflammation.

#### *TRPV1 G564S knock-in mice exhibit dramatically reduced histamine-evoked scratching behaviors*

It is well known that TRPV1 contributes to histamine-induced itch signal transmission. To check whether the gain-of-function mutation in TRPV1 affects itch signaling, we intradermally injected six prototypical pruritogens into the nape of mice and counted the number of scratching bouts in 30 min. Intradermal injection of PBS did not induce scratching behavior (data not shown). After injection of chloroquine, ET-1, 5-HT, SLIGRL, or compound 48/80, scratching responses did not significantly differ between TRPV1 G564S<sup>+/+</sup> mice and wild-type littermates, whereas a marked reduction in histamine-induced scratching bouts occurred in TRPV1 G564S<sup>+/+</sup> mice (Figure 5(a) and (b)), indicating that the TRPV1 gain-of-function mutation impairs histamine-dependent itch sensation.

#### *TRPV1 G564S mutation attenuates functional TRPV1 phosphorylation and surface targeting*

The data from electrophysiology, calcium imaging, and behavioral assessment demonstrated that the TRPV1 G564S mutation stabilizes the open conformation and causes a sustained inactive state similar to the agonist-

induced desensitization which is characterized by the inability of the receptor to respond to capsaicin or other noxious stimuli. To determine the underlying mechanisms, we first examined the total amount of TRPV1 protein in acutely dissociated DRG neurons. Western blot analysis showed no significant difference in TRPV1 protein level between TRPV1 G564S<sup>+/+</sup> mice and wild-type littermates (Figure 1(d)), suggesting that the role of the G564S mutation in TRPV1 functions is not related to the overall TRPV1 expression.

Prior studies have reported that TRPV1 is activated and then Ca<sup>2+</sup> ions enter the cell, stimulating calcium-dependent signaling mechanisms, including dephosphorylation of TRPV1, thereby desensitizing the receptor. Thus, we further evaluated the effect of the G564S mutation on TRPV1 phosphorylation. HEK293a cells were transfected with HA-TRPV1 or HA-TRPV1-G564S plasmids, and the level of phosphorylated TRPV1 was measured by immunoprecipitation followed with Western blot analysis. We found that the G564S mutation

significantly reduced the level of phosphorylated TRPV1 compared with the wild-type group (Figure 6(a)). The ratio of phosphorylated protein to total TRPV1 in the TRPV1 G564S group was reduced to  $73.30 \pm 3.57\%$  of the wild-type group (Figure 6(b)). This result indicates that the mutation of Gly-564 to serine effectively attenuates TRPV1 phosphorylation, which is critical for TRPV1 sensitization.

Researchers have recently discovered that the disruption of the surface targeting of TRPV1 attenuates thermal hyperalgesia. To address whether the G564S mutation affects TRPV1 membrane trafficking, we measured the level of surface TRPV1 in HEK293a cells co-expressing HA with either wild-type TRPV1 or the G564S mutant using surface biotinylation assays. The results showed that the G564S mutation substantially decreased the surface TRPV1 levels when there was no difference in total TRPV1 expression between the two groups (Figure 6(c)). The ratio of surface-to-total TRPV1 in the TRPV1 G564S group was reduced to

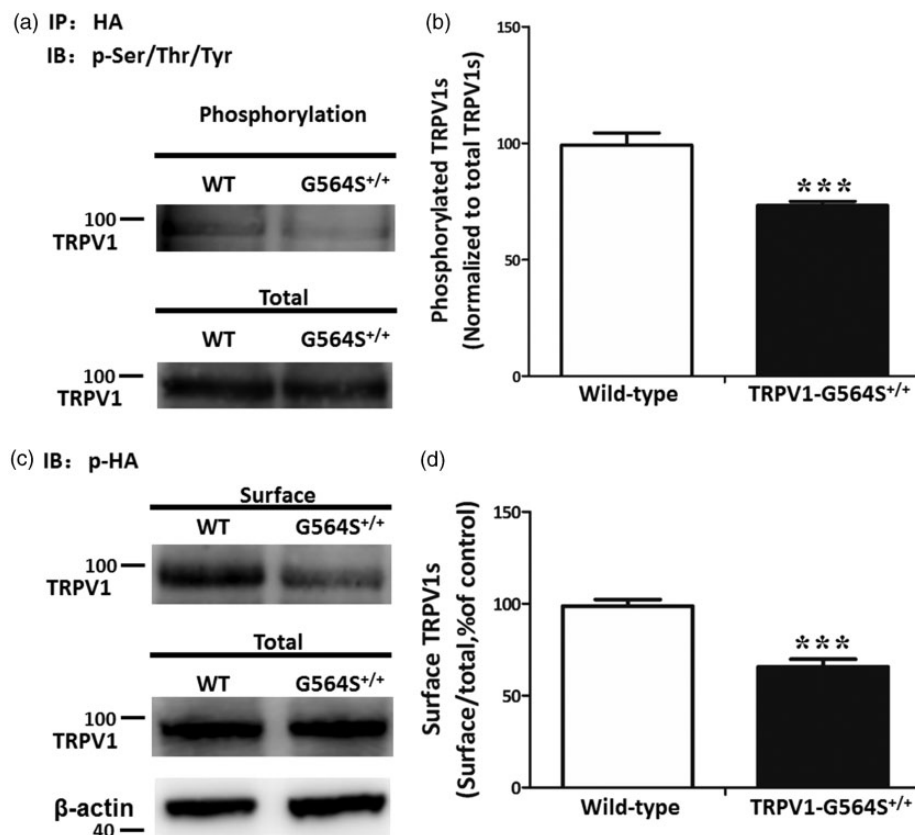


**Figure 6.** Reduced phosphorylation and membrane localization of TRPV1 channels caused by G564S mutation. (a) Western blots showing the phosphorylated TRPV1 protein levels in HEK293a cells transfected with HA-TRPV1 or HA-TRPV1-G564S plasmids after immunoprecipitation by anti-HA antibody. (b) Analysis showing a significantly lower phosphorylation level of the TRPV1 G564S channel than the wild type control. Error bars, SEM; \*\*\**p* < 0.001, unpaired Student's *t* test. All experiments were repeated at least four times. (c) Surface biotinylation assays for the amount of TRPV1 at the cell surface. (d) Analysis showing the ratio of surface to total TRPV1 normalized to the wild-type control. Error bars, SEM; \*\*\**p* < 0.001, unpaired Student's *t* test. All experiments were repeated at least four times. TRPV: transient receptor potential vanilloid; HA: hemagglutinin; WT: wild type.

$65.76 \pm 8.12\%$  of the wild-type control (Figure 6(d)). Taken together, these results indicate that the G564S mutant effectively reduces TRPV1 phosphorylation and surface targeting, which attenuates channel functions.

## Discussion

The topology of TRPV1 is homologous to that of other TRP channels, each of which is assembled as a homotrimer with each subunit containing six TM segments and intracellularly located N- and C-termini. The Gly564 is located in the linker between TM4 and TM5 of mouse TRPV1, where the TM4–5 linker helix is thought to couple with the inner helix of the TM6 segment to dilate (open) and constrict (close) the pore entryway.<sup>6</sup> Point mutations of TRPV3 at Gly573 to Ser/Cys, which aligns with Gly564 in mouse TRPV1, render the channel spontaneously active under normal physiological conditions, thus altering ion homeostasis and the membrane potential of skin keratinocytes, leading to hair loss and dermatitis-like skin diseases.<sup>7,16</sup> Therefore, we hypothesized that the G564S mutation in mouse TRPV1 enhances channel activity and results in certain severe diseases. We have characterized the functional properties of the G564S mutant via inside-out and whole-cell patch-clamp recordings in transiently transfected HEK293a cells. Consistent with a prior study on the rat G563S mutant expressed in HEK293t cells,<sup>8</sup> the G564S mutation in mouse TRPV1, corresponding to rat TRPV1 G563S, modulated the gating of the TRPV1 channel by shifting the voltage dependence toward more negative membrane potentials. In addition, the G564S mutation increased the basal current under physiological conditions and dramatically altered the desensitization of capsaicin-activated currents through TRPV1. The electrophysiological results demonstrated that the G564S mutation results in TRPV1 gain of function.

TRPV1 is a polymodal receptor for a wide spectrum of physical (noxious heat and pressure) and chemical (protons, irritants, and inflammatory mediators) stimuli, and it exhibits high selectivity for capsaicin.<sup>17</sup> A gain-of-function mutation in an ion channel may enhance the responses to one type of stimulus, but sensitivity to other agonists may remain unchanged or even get diminished. Xiao et al. have provided *in vitro* evidence that point mutations of mouse TRPV3 at Gly573 to Ser/Cys abolish the channel response to thermal and chemical stimuli.<sup>16</sup> Another study of G563S mutation in rat TRPV1 shows slow activation kinetics and incomplete deactivation after capsaicin washout.<sup>8</sup> Here, electrophysiological studies showed that the current amplitudes evoked by the first capsaicin application were significantly reduced in HEK293a cells expressing the G564S mutant, compared with wild-type TRPV1, supporting the concept

that the residue at position 564 is important for capsaicin sensitivity. We further examined the effect of the gain-of-function mutation on capsaicin sensitivity in DRG neurons using fura-2 AM-based  $\text{Ca}^{2+}$  imaging and found that a single Gly-to-Ser substitution at position 564 (G564S) resulted in a significant reduction in capsaicin-evoked  $\text{Ca}^{2+}$  influx. Finally, TRPV1 G564S<sup>+/+</sup> mice exhibited impaired behavioral responses to capsaicin. Together, these data demonstrate that the TRPV1 G564S mutation causes a dramatic reduction in capsaicin sensitivity both *in vitro* and *ex vivo*. However, note that two capsaicin applications to the TRPV1 G564S channel induced similar current amplitudes in the electrophysiological study, implying that the gain-of-function mutation contributes to the absence of capsaicin-induced receptor desensitization in the TRPV1 G564S mutant. A possible explanation for this phenomenon is that the gain-of-function mutation may easily lead to TRPV1 desensitization and thus reduce capsaicin sensitivity. The roles of TRPV1 in pain and neurogenic inflammation have been very well covered in previous studies. TRPV1 is an important detector of noxious heat under normal conditions and is also a central mediator of inflammatory heat hyperalgesia.<sup>2,9,10,18</sup> TRPV1 knock-out mice are impaired in the detection of painful heat and exhibit little thermal hypersensitivity during inflammation.<sup>9</sup> Interestingly, the previous *in vitro* studies showed that the G563S mutant in rat TRPV1 showed impaired temperature sensitivity.<sup>19,20</sup> Similarly, TRPV1 G564S<sup>+/+</sup> mice exhibited marked deficits in their behavioral responses to noxious thermal stimuli. In addition, we found that TRPV1 G564S<sup>+/+</sup> mice displayed a clear inhibition of thermal hyperalgesia after CFA-induced inflammation. Together, in contrast to what is shown in the electrophysiological study, our behavioral data have demonstrated that the gain-of-function mutation in TRPV1 unexpectedly attenuates the channel heat response under normal and inflammatory conditions. A good hypothesis to reconcile this contradiction is that impaired behavioral responses may be mostly derived from the secondary effects of the mutation. Gain of function of TRPV1 conversely results in compensatory desensitization, which may be a critical biological defense mechanism to protect sensory neurons from potential harmful consequences.

TRPV1 has been reported to mediate histamine-evoked inward currents and the intracellular  $\text{Ca}^{2+}$  increase in sensory neurons. Mice lacking TRPV1 exhibit markedly reduced histamine-induced itching,<sup>21</sup> though the role of the TRPV1 channel in histamine-independent itch appears controversial. Herein, our results showed that TRPV1 G564S<sup>+/+</sup> mice displayed robust deficits in histamine-evoked scratching behavior but normal reactivity to histamine-independent itch stimuli,

indicating that the gain-of-function mutation in TRPV1 is responsible only for histamine-induced itching.

The signaling events involved in TRPV1 functional changes have been extensively investigated. Previous studies have indicated that the total amount of TRPV1 channels in neurons, especially primary sensory neurons, regulates channel sensitivity.<sup>22</sup> Therefore, we evaluated the TRPV1 protein levels in DRGs isolated from TRPV1 G564S<sup>+/+</sup> mice and their wild-type littermates but found no difference between them.

Ca<sup>2+</sup>-dependent phosphorylation and dephosphorylation processes are involved in regulating the desensitization and excitability of TRPV1 channels.<sup>23–25</sup> In addition, subcellular transport from vesicles to the plasma membrane has recently been reported to alter the TRPV1 activation threshold and affect heat pain sensitivity and hyperalgesia.<sup>26,27</sup> Our results indicated that the gain-of-function mutation in TRPV1 caused a significant increase in the basal intracellular Ca<sup>2+</sup> concentration, leading to a significant reduction in TRPV1 phosphorylation of serine/threonine and tyrosine residues, a mechanism similar to the Ca<sup>2+</sup>-dependent desensitization of TRPV1 channels. We did not, however, distinguish serine phosphorylation of TRPV1 from that of threonine or tyrosine residues. Moreover, surface biotinylation assays demonstrated that the G564S mutation significantly attenuated functional TRPV1 membrane targeting. Since decreased phosphorylation and surface levels of TRPV1 have been associated with reduced channel activity, these results can explain the dramatically reduced TRPV1 responses to thermal and chemical stimuli such as capsaicin in the G564S mutant.

In conclusion, we have generated a mouse model with a gain-of-function mutation in TRPV1, wherein the pain and histamine-dependent itch sensations are impaired due to decreased phosphorylation levels and reduced membrane localization of TRPV1. TRPV1 G564S knock-in mice thus provide an appropriate animal model to study TRPV1 channel functions under different conditions as well as the underlying molecular mechanisms.

### Authors' Note

The current address of Dr Lina Duo is Department of Dermatology, Chengdu Integrated TCM & Western Medicine Hospital, Chengdu, China and Department of Dermatology, Chengdu First People's Hospital, Chengdu, China.

### Author Contributions

YY and YW designed research. LD, LH, NT, GC, and HW performed experiments. LD, LH, NT, and ZL analyzed data. LD, LH, and NT wrote the manuscript.

### Acknowledgment

The authors thank Dr Zhuan Zhou (Institute of Molecular Medicine, Peking University) for providing a mouse TRPV1 plasmid and Dr Iain C Bruce (Institute of Molecular Medicine, Peking University) for helpful comments on the manuscript.

### Declaration of Conflicting Interests

The author(s) declared no potential conflicts of interest with respect to the research, authorship, and/or publication of this article.

### Funding

The author(s) disclosed receipt of the following financial support for the research, authorship, and/or publication of this article: This work was supported by the China National Funds for Distinguished Young Scientists (grant 81425020 to YY) and National Natural Science Foundation of China (grant 81271744 to YY).

### ORCID iD

Lina Duo  <http://orcid.org/0000-0003-4742-8293>

### References

1. Szallasi A and Blumberg PM. Vanilloid receptors: new insights enhance potential as a therapeutic target. *Pain* 1996; 68: 195–208.
2. Caterina MJ, Schumacher MA, Tominaga M, Rosen TA, Levine JD and Julius D. The capsaicin receptor: a heat-activated ion channel in the pain pathway. *Nature* 1997; 389: 816–824.
3. Tominaga M, Caterina MJ, Malmberg AB, Rosen TA, Gilbert H, Skinner K, Raumann BE, Basbaum AI and Julius D. The cloned capsaicin receptor integrates multiple pain-producing stimuli. *Neuron* 1998; 21: 531–543.
4. Voets T, Droogmans G, Wissenbach U, Janssens A, Flockerzi V and Nilius B. The principle of temperature-dependent gating in cold- and heat-sensitive TRP channels. *Nature* 2004; 430: 748–754.
5. Latorre R, Zaelzer C and Brauchi S. Structure-functional intimacies of transient receptor potential channels. *Quart Rev Biophys* 2009; 42: 201–246.
6. Liao M, Cao E, Julius D and Cheng Y. Structure of the TRPV1 ion channel determined by electron cryo-microscopy. *Nature* 2013; 504: 107–112.
7. Lin Z, Chen Q, Lee M, Cao X, Zhang J, Ma D, Chen L, Hu X, Wang H, Wang X and Zhang P. Exome sequencing reveals mutations in TRPV3 as a cause of Olmsted syndrome. *Am J Hum Genet* 2012; 90: 558–564.
8. Boukalova S, Touska F, Marsakova L, Hynkova A, Sura L, Chvojka S, Dittert I and Vlachova V. Gain-of-function mutations in the transient receptor potential channels TRPV1 and TRPA1: how painful? *Physiol Res* 2014; 63: S205–S213.
9. Caterina MJ, Leffler A, Malmberg AB, Martin WJ, Trafton J, Petersen-Zeitl KR, Koltzenburg M, Basbaum AI and Julius D. Impaired nociception and pain sensation



- in mice lacking the capsaicin receptor. *Science (New York, NY)* 2000; 288: 306–313.
10. Davis JB, Gray J, Gunthorpe MJ, Hatcher JP, Davey PT, Overend P, Harries MH, Latcham J, Clapham C, Atkinson K and Hughes SA. Vanilloid receptor-1 is essential for inflammatory thermal hyperalgesia. *Nature* 2000; 405: 183–187.
  11. Yang P and Zhu MX. TRPV3. *Handb Exp Pharmacol* 2014; 222: 273–291.
  12. Sakurada T, Katsumata K, Tan-No K, Sakurada S and Kisara K. The capsaicin test in mice for evaluating tachykinin antagonists in the spinal cord. *Neuropharmacology* 1992; 31: 1279–1285.
  13. Patel KN, Liu Q, Meeker S, Udem BJ and Dong X. Pirt, a TRPV1 modulator, is required for histamine-dependent and -independent itch. *PLoS One* 2011; 6: e20559
  14. Li Y, Hu F, Chen HJ, Du YJ, Xie ZY, Zhang Y, Wang J and Wang Y. LIMK-dependent actin polymerization in primary sensory neurons promotes the development of inflammatory heat hyperalgesia in rats. *Sci Signal* 2014; 7: ra61
  15. Mohapatra DP and Nau C. Desensitization of capsaicin-activated currents in the vanilloid receptor TRPV1 is decreased by the cyclic AMP-dependent protein kinase pathway. *J Biol Chem* 2003; 278: 50080–50090.
  16. Xiao R, Tian J, Tang J and Zhu MX. The TRPV3 mutation associated with the hairless phenotype in rodents is constitutively active. *Cell Calcium* 2008; 43: 334–343.
  17. Vennekens R, Owsianik G and Nilius B. Vanilloid transient receptor potential cation channels: an overview. *Curr Pharm Des* 2008; 14: 18–31.
  18. Szallasi A, Cortright DN, Blum CA and Eid SR. The vanilloid receptor TRPV1: 10 years from channel cloning to antagonist proof-of-concept. *Nat Rev Drug Discov* 2007; 6: 357–372.
  19. Boukalova S, Marsakova L, Teisinger J and Vlachova V. Conserved residues within the putative S4-S5 region serve distinct functions among thermosensitive vanilloid transient receptor potential (TRPV) channels. *J Biol Chem* 2010; 285: 41455–41462.
  20. Boukalova S, Teisinger J and Vlachova V. Protons stabilize the closed conformation of gain-of-function mutants of the TRPV1 channel. *Biochim Biophys Acta* 2013; 1833: 520–528.
  21. Shim WS, Tak MH, Lee MH, Kim M, Kim M, Koo JY, Lee CH, Kim M and Oh U. TRPV1 mediates histamine-induced itching via the activation of phospholipase A2 and 12-lipoxygenase. *J Neurosci* 2007; 27: 2331–2337.
  22. Ji RR, Samad TA, Jin SX, Schmoll R and Woolf CJ. p38 MAPK activation by NGF in primary sensory neurons after inflammation increases TRPV1 levels and maintains heat hyperalgesia. *Neuron* 2002; 36: 57–68.
  23. Bhawe G, Zhu W, Wang H, Brasier DJ, Oxford GS and Gereau RW IV. cAMP-dependent protein kinase regulates desensitization of the capsaicin receptor (VR1) by direct phosphorylation. *Neuron* 2002; 35: 721–731.
  24. Rathee PK, Distler C, Obreja O, Neuhuber W, Wang GK, Wang SY, Nau C and Kress M. PKA/AKAP/VR-1 module: A common link of Gs-mediated signaling to thermal hyperalgesia. *J Neurosci* 2002; 22: 4740–4745.
  25. Zhuang ZY, Xu H, Clapham DE and Ji RR. Phosphatidylinositol 3-kinase activates ERK in primary sensory neurons and mediates inflammatory heat hyperalgesia through TRPV1 sensitization. *J Neurosci* 2004; 24: 8300–8309.
  26. Sanz-Salvador L, Andres-Borderia A, Ferrer-Montiel A and Planells-Cases R. Agonist- and  $Ca^{2+}$  dependent desensitization of TRPV1 channel targets the receptor to lysosomes for degradation. *J Biol Chem* 2012; 287: 19462–19471.
  27. Xing BM, Yang YR, Du JX, Chen HJ, Qi C, Huang ZH, Zhang Y and Wang Y. Cyclin-dependent kinase 5 controls TRPV1 membrane trafficking and the heat sensitivity of nociceptors through KIF13B. *J Neurosci* 2012; 32: 14709–14721.